



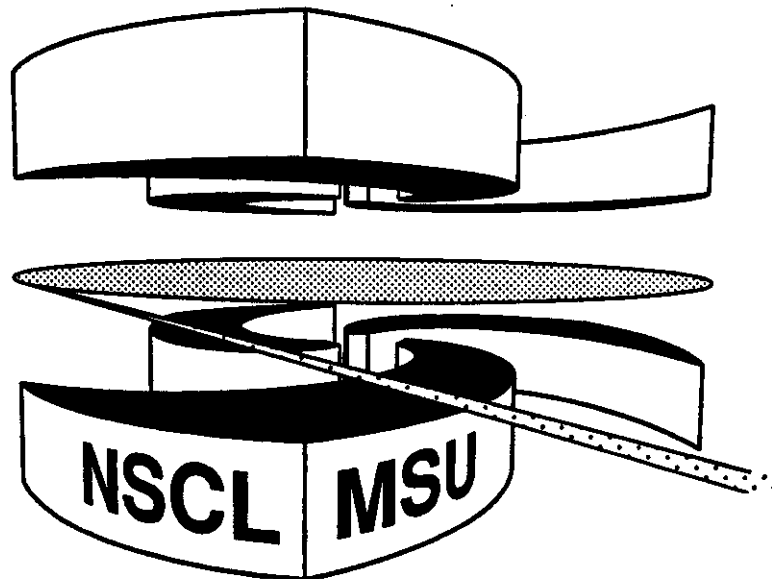
Michigan State University

National Superconducting Cyclotron Laboratory

**NUCLEAR DISSIPATION AND
THE GIANT DIPOLE RESONANCE**

M. THOENNESSEN and J.R. BEENE

**Invited talk presented at the Symposium on Reflections
and Directions in Low Energy Heavy Ion Physics, Oak Ridge,
14-15 October 1991, to be published by World Scientific.**



NUCLEAR DISSIPATION AND THE GIANT DIPOLE RESONANCE

M. THOENNESSEN

*National Superconductin Cyclotron Laboratory and
Department of Physics and Astronomy,
Michigan State University, East Lansing, Michigan 48824*

and

J. R. BEENE

Oak *Ridge* National Laboratory, Oak *Ridge, Tennessee* 37831

The influence of nuclear dissipation on the formation and decay of compound nuclei is studied with the γ -ray decay of the giant dipole resonance (GDR) built on highly excited states. The compound nuclei ^{164}Yb , ^{160}Er , and ^{110}Sn were produced with very mass-asymmetric and with more mass-symmetric target/projectile combinations. While the γ -ray spectra from the more symmetrically formed ^{160}Er and ^{164}Yb show large deviation from statistical model prediction, the reaction leading to ^{110}Sn show no such deviations. We discuss a possible explanation of these observed entrance channel effects qualitatively within the particle exchange model.

1. Introduction

The fusion of heavy nuclei is known to be much more complex than it appeared in the early days of heavy-ion physics. Most of the early fusion data could be accounted for very well by simple static one dimensional potential models.¹ However about a decade ago, the importance of dynamical effects began to be appreciated. Two very striking (and superficially contradictory) effects have been extensively documented: 1) Fusion induced by heavy beams below the nominal Coulomb barrier is generally very much enhanced beyond prediction of static one dimensional barrier penetration models.² 2) Exceeding the one dimensional potential energy barrier is not enough to ensure fusion: under certain conditions a so called "extra push" is required.³ Both these effects depend on the dynamics of the fusion process. The extra push effect was predicted in a series of papers published about ten years ago by Swiatecki and collaborators exploring the effects of dissipative dynamics on heavy-ion reactions.⁴ Many effects of dissipation have been studied experimentally over the last decade.

Once the reactants pass inside a saddle point in the complex multi-dimensional configuration space describing the reaction, fusion is considered to have occurred. The system is then expected to evolve rapidly toward an equilibrated compound nucleus. One would expect, in general, that dynamical effects could influence this evolution toward equilibrium, however, the time scale for the equilibration has generally been

assumed to be so fast compared to any decay processes relevant to the compound system (at the moderate excitation energies reached in near barrier reactions) that such dynamical influences can be ignored. Once the equilibrated compound system is reached, the Bohr independence hypothesis should apply, so that the subsequent decay is correctly treated by a conventional statistical model, and is therefore independent of the way the system was formed.

One aspect of dissipative dynamics is known to influence the compound nucleus decay. Neutron multiplicity measurements in heavy systems observed an enhancement of neutrons evaporated prior to fission compared to the statistical model.⁵ This effect has been explained with dissipation which slows down the fission process allowing for additional particle and γ -ray emission before fission.⁶

Recent measurements of the fusion of nearly symmetric systems near the Coulomb barrier (where both the effects mentioned above can be simultaneously relevant) have raised the possibility that dynamics, or perhaps some other effect sensitive to the entrance channel asymmetry, is influencing the decay of the fused system in a way that seems to violate the independence hypothesis. These effects were also first observed in neutron multiplicity measurements.^{7,8} When the compound nucleus is formed using projectile target combinations with different mass asymmetries, at the same excitation energy and the same angular momentum, differences in the neutron multiplicity were observed. This observation is still controversial, and not adequately understood.

We will describe experiments that use a different probe to study these entrance channel effects. The γ -ray decay of the giant dipole resonance (GDR) built on highly excited states turns out to be a very sensitive tool to study any dissipative effects. It was shown early on in the study of γ -ray spectra in the GDR region that γ rays from the GDR are emitted predominantly during the first few decay steps of the compound nucleus,⁹ thus it should be sensitive to effects during the formation and first stages of the decay. In addition, the γ -ray spectrum exhibits a splitting of the GDR for deformed nuclei which can be related in a straightforward way to the shape of the nucleus. This is important because the fusion process, like fission, involves dramatic changes in the shape of the nucleus.

In this paper we present γ -ray spectra relevant to these entrance channel effects in different mass regions and try to explain them qualitatively within a dynamical fusion model.

2. Experiments

The experiments were performed using ion beams from the Holifield Heavy Ion Research Facility tandem at Oak Ridge National Laboratory. Self-supporting metal targets were placed inside the Spin Spectrometer.¹⁰ Details of the reactions are listed in Table I. High-energy γ -rays (6 - 25 MeV) were detected with the Oak Ridge BaF₂ array of four close-packed clusters of 19 hexagonal detectors each; the individual detectors were 6.5 cm face to face and 20 cm long. The clusters were positioned at 21°, 63° (two), and 117°, at distances from the target of 57 cm and 77 cm for the backward

and forward angles, respectively. At these positions NaI detectors were removed from the Spin-Spectrometer structure. An additional cluster of 19 detectors from Michigan State University was added for the reactions forming the ^{110}Sn compound nucleus at 18° with similar dimensions (25 cm long, 6 cm face to face) at the forward angle in order to increase the solid angle.

Table I

Summary of measured reactions. The columns contain: the reaction, the compound nucleus (CN), the beam energy, the excitation energy corrected for energy loss in the target, and the maximum angular momentum.

Reaction	CN	E_{beam} (MeV)	E_{CN}^* (MeV)	$J_{max}(\hbar)$
$^{16}\text{O} + ^{144}\text{Nd}$	^{160}Er	86.3	53	30
$^{64}\text{Ni} + ^{96}\text{Zr}$	^{160}Er	236.6	53	44
$^{16}\text{O} + ^{148}\text{Sm}$	^{164}Yb	82.8	49	30
$^{64}\text{Ni} + ^{100}\text{Mo}$	^{164}Yb	236.6	49	44
$^{18}\text{O} + ^{92}\text{Mo}$	^{110}Sn	71.6	56	30
$^{50}\text{Ti} + ^{60}\text{Ni}$	^{110}Sn	163.2	56	30

The experiments were performed with a dc beam, and neutron - γ -ray separation was achieved by timing the BaF_2 array against an average time deduced from at least three low-energy γ -ray transitions detected in the Spin Spectrometer.^{11,12} The γ -ray energies within each cluster were summed after gain matching and neutron separation in order to improve the detector response. The total γ -ray spectrum is then the sum of the four (five) individual cluster spectra. The spin spectrometer was used as a multiplicity filter to gate on reactions that lead to angular momenta of 15 - 30 \hbar . This was necessary due to the different maximum angular momenta in the two ^{64}Ni reactions as listed in Table I and shown in Fig. 1. More experimental details are described elsewhere.¹²

3. Gamma-ray Spectra and Standard Statistical Model Calculations

Figure 2 shows the total γ -ray spectra for the four reactions leading to ^{160}Er (a) and ^{164}Yb (b). The γ -ray spectra are normalized between 6 and 7 MeV. While the ^{16}O reactions show the features expected from earlier work, including a typical GDR bump at 13 MeV as expected, the ^{64}Ni induced reactions exhibit large differences.

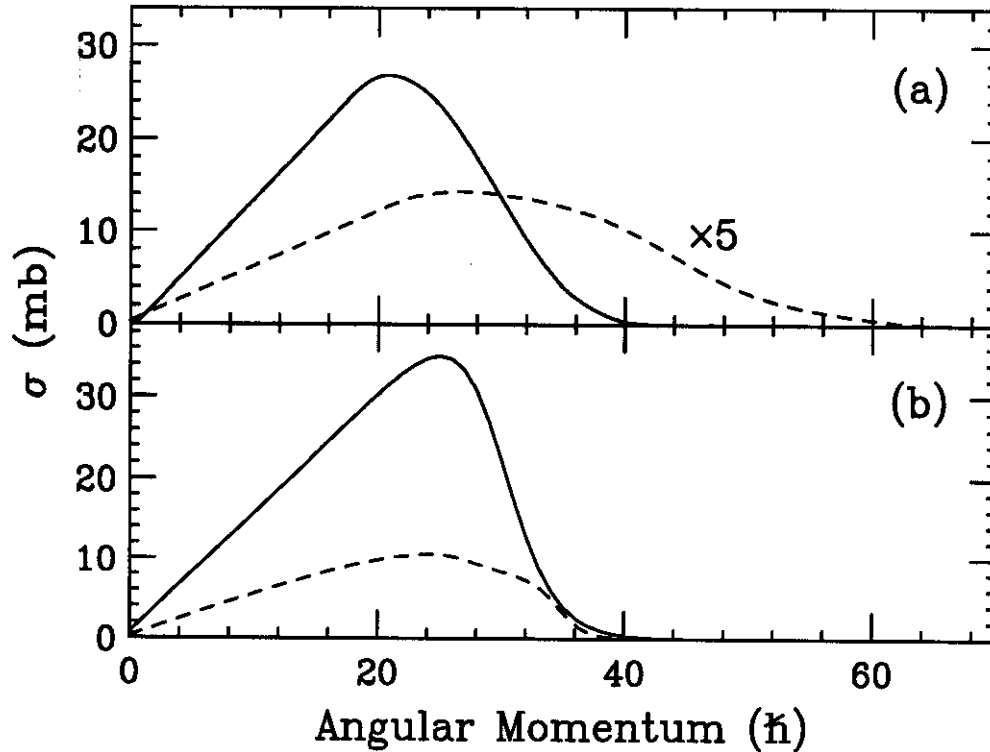


Figure 1: Distributions of angular momenta populated in the different reactions forming the compound nuclei ^{164}Yb (a) and ^{110}Sn (b). The solid curves correspond to the asymmetric reactions, $^{16}\text{O} + ^{148}\text{Sm}$ (a), $^{18}\text{O} + ^{92}\text{Mo}$ (b), and the dashed curves to the more symmetric reactions, $^{64}\text{Ni} + ^{100}\text{Mo}$ (a), $^{50}\text{Ti} + ^{60}\text{Ni}$ (b).

Details of the data analysis can be found in Ref. 12. The present γ -ray spectra are different from the previously published data, because a better cosmic ray rejection was applied.

The solid lines in Fig. 2 are statistical model calculations using the computer code CASCADE.¹³ The entrance channel angular momentum distribution was taken from experimental data.^{11,14,15} Only the decay of the angular momentum population between 15 and 30 \hbar was calculated accounting for the multiplicity cuts applied to the data. The level density parameter was chosen to be $a=A/10$. The calculations were folded with the response function for the BaF_2 arrays calculated with codes based on GEANT.¹⁶ The GDR strength was represented by two lorentzian peaks at energies of $E_1 = 12.4$ MeV and $E_2 = 15.7$ MeV for ^{160}Er and $E_1 = 12.0$ MeV and $E_2 = 16.2$ MeV for ^{164}Yb . The widths of the two components were $\Gamma_1 = 4.9$ MeV for ^{164}Yb (5.3 MeV for ^{160}Er) and $\Gamma_2 = 7.2$ MeV. Those values are in general agreement with previous GDR experiments in this mass region.¹⁷

One major concern is the contribution of reactions other than fusion, as the data were not gated on evaporation residues. However, the various inelastic reactions which might be significant typically produce nuclei at excitation energies much lower

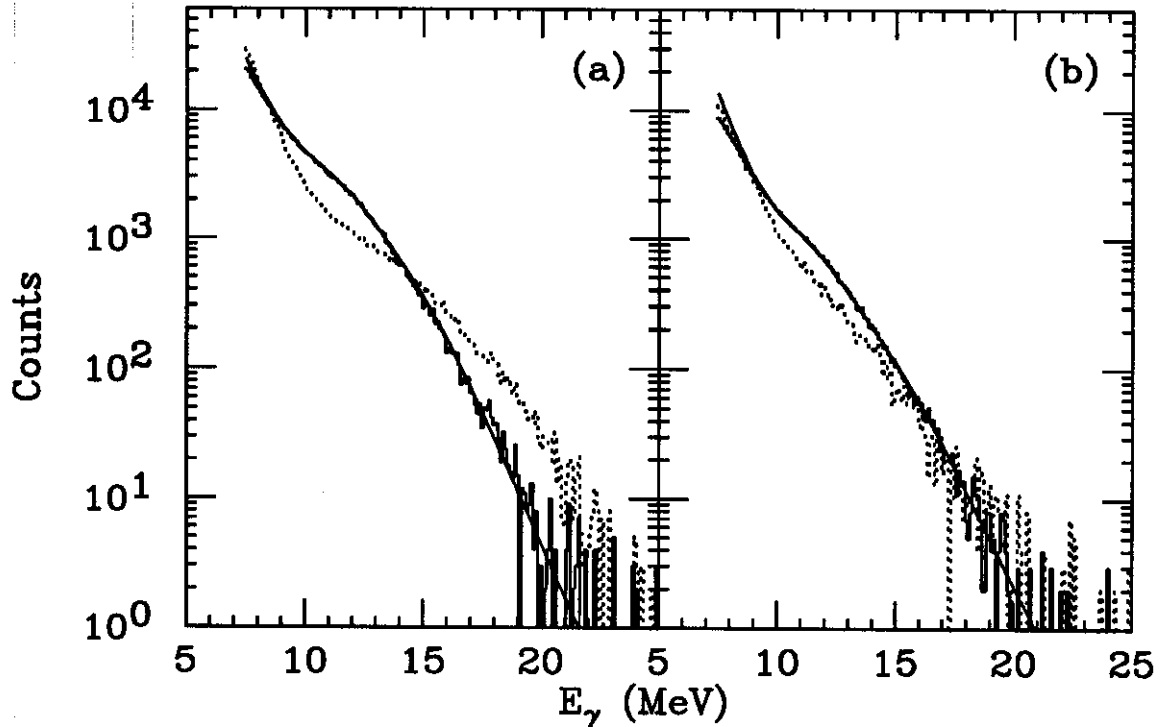


Figure 2: Gamma-ray spectra of the compound nucleus decay of ^{160}Er (a) and ^{164}Yb (b). The histograms correspond to the ^{16}O (solid) and ^{64}Ni (dashed) induced reactions. The solid curves are fits from statistical model calculations.

than the ~ 50 MeV of the fused systems, and at low spins so that the cut in angular momentum space should discriminate against those events. The most significant contributions are likely to come from deep inelastic collisions in the ^{64}Ni induced reactions, but even these will produce residual nuclei at low spin and excitation energy, since these reactions are just above their Coulomb barriers.¹⁸

Obviously, the large differences observed in the ^{64}Ni induced reaction cannot be accounted for within reasonable changes of the statistical model parameters. An attempt to fit the γ -ray spectra from the ^{64}Ni induced reactions, leads to a strongly reduced integrated strength for the GDR compared to the 100% of the Thomas Reiche Kuhn (TRK) sum rule that was used in the asymmetric cases. Gamma-ray spectra of previous experiments with heavy projectiles at higher energies could be described within the statistical model, so that the large discrepancies we observe must be related to the near barrier formation of the compound nuclei.¹⁹

However, the present data are controversial; recently Fornal *et al.*²⁰ published results of similar measurements forming the compound nucleus ^{156}Er with $^{64}\text{Ni} + ^{92}\text{Zr}$ and $^{12}\text{C} + ^{144}\text{Sm}$. Fornal *et al.* claim to observe no differences between the two γ -ray spectra and thus no evidence for entrance channel effects. However, a closer comparison of the γ -ray spectra induced with ^{12}C and ^{64}Ni actually reveals similar structural differences that are shown in Fig. 2. In addition, the GDR strength

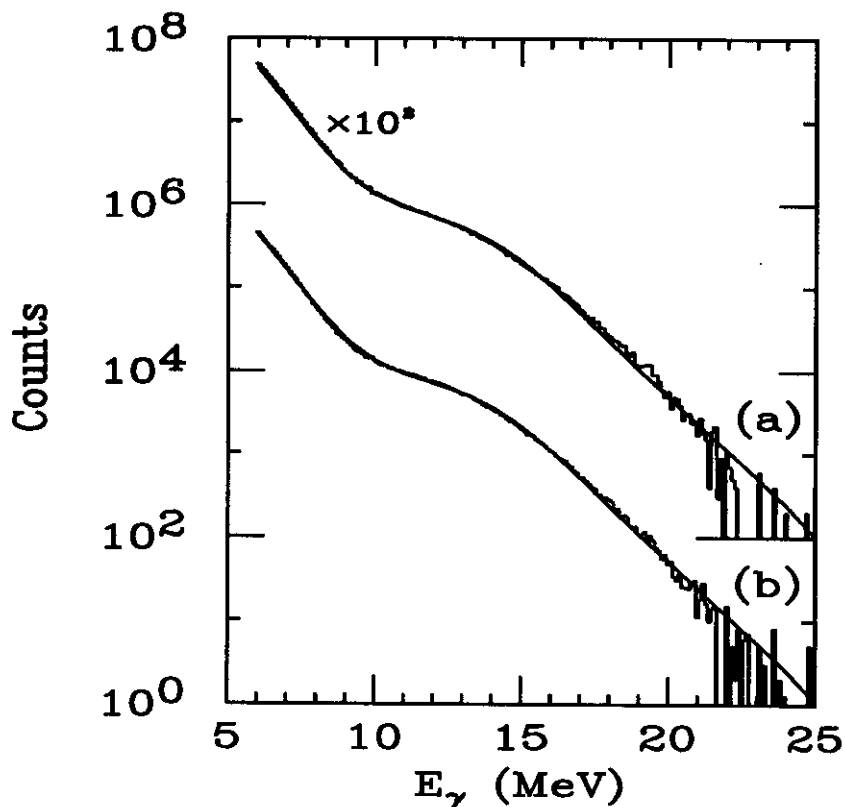


Figure 3: Gamma-ray spectra from the decay of ^{110}Sn . The histograms correspond to the data following ^{60}Ti (a) and ^{18}O (b) induced reactions and the solid curves are fits from statistical model calculations.

parameters quoted in Ref. 20 show large unexplained differences. The γ -ray spectra from the ^{12}C and the ^{64}Ni reaction were fitted with strengths of 180% (!) and 91% of the TRK sum rule respectively. This discrepancy certainly points toward differences in the spectral shape similar to those shown in Fig. 2. The reduced GDR strength in the ^{64}Ni case agrees with the suggested fit parameters mentioned earlier.

Evidence for entrance channel effects was also observed in γ -ray measurements of highly excited neutron deficient thorium isotopes.²¹ The γ -ray strength from the GDR decreased when the compound nucleus was formed with more symmetric projectiles (^{16}O , ^{24}Mg and ^{32}S).

Due to the controversy in the $^{160}\text{Er}/^{164}\text{Yb}$ mass region and the considerable interest in the entrance channel effect, we measured a system in a different mass region. Figure 3 shows the γ -ray spectra following the reactions $^{50}\text{Ti} + ^{60}\text{Ni}$ (a) and $^{18}\text{O} + ^{92}\text{Mo}$ (b) forming the compound nucleus ^{110}Sn at 56 MeV. This system is known to be spherical even at higher temperatures and should exhibit a GDR strength function with a single lorentzian peak, making entrance channel effects easier to detect.²²

Figure 3 reveals that the two γ -ray spectra are essentially identical. Again, the data were gated on the same spin range, which in this case is not as crucial (Table I, Fig. 1) as in the $^{160}\text{Er}/^{164}\text{Yb}$ mass region. CASCADE calculations with the same

statistical model parameters except for the GDR parameters were performed and folded with the response function. As expected the spectra could be fitted with a single lorentzian strength function with $E_{GDR} = 14.7$ MeV and $\Gamma_{GDR} = 6.5$ MeV, again in good agreement with previously measured data.^{22,23} Both, the ^{18}O and the ^{60}Ti induced reaction could be fitted with the same parameters, thus showing no sign of the existence of entrance channel effects in this mass region.

In the following we try to relate the seemingly contradictory observations to reaction dynamics including nuclear dissipation.

4. Nuclear Dissipation Effect

The differences between different entrance channels reported in the previous section can not be explained within the standard statistical model. One obvious possibility is to search for the origin of the differences in the dynamics of the formation of the compound nucleus. To do this we should try to investigate the time evolution of the parameters which are most crucial in influencing compound nucleus decay such as the excitation energy and the shape (which can be especially important for the γ -ray decay spectra).

Before we proceed to the time evolution, it is useful for orientation to consider semi-quantitative arguments presented by Swiatecki⁴ which provide broad guidance as to when dissipative dynamical effects might be significant for fusion-like reactions. Figure 4 is a plot of the relative fissility, defined as $X_0 = Z^2 e^2 / (16\pi\gamma R^3)$ versus the entrance channel asymmetry $\Delta = (R_1 - R_2) / (R_1 + R_2)$ where γ is the surface-energy coefficient. A line is drawn indicating the contour along the effective fissility $x = 0.57$ ($x = X_0 \cdot (1 - \Delta^2) / (1 + 3\Delta^2)$). This value of x is referred to as the critical fissility (x_c) since for $x < x_c$ dissipative effects are expected to be small: a system whose kinetic energy exceeds the static interaction barrier should proceed very rapidly to the equilibrated compound system. However for $x > x_c$ dissipative effects impede fusion: the dynamical evolution toward an equilibrated system should be slower. The "extra push" effect alluded to in Section 1, and deep inelastic collision should start to contribute significantly to the total reaction cross section even for small impact parameters and just above the interaction barrier. We should note that the value $x_c = 0.57$ was proposed by Swiatecki on theoretical grounds: subsequent experiments concentrating on the extra push effect indicate $x_c \sim 0.7$.²⁴ On the other hand the appearance of significant deep inelastic yield near the Coulomb barrier has been noted for x close to 0.57. The values in Fig. 4 correspond to angular momentum of $l = 0$. For larger angular momenta the critical fissility is reduced. At any rate, Fig. 4 serves to indicate qualitatively that in the region to the right of and below the $x = x_c$ line, dissipative dynamical effects can be expected to be significant. One immediately sees that only the ^{64}Ni induced reactions are located in this extra push region, and even though the $^{50}\text{Ti} + ^{60}\text{Ni}$ reaction is even more symmetric, the low fissility of this system pushes it quite far outside the dissipative region.

Feldmeier incorporated Swiatecki's ideas of macroscopic dissipative dynamics into

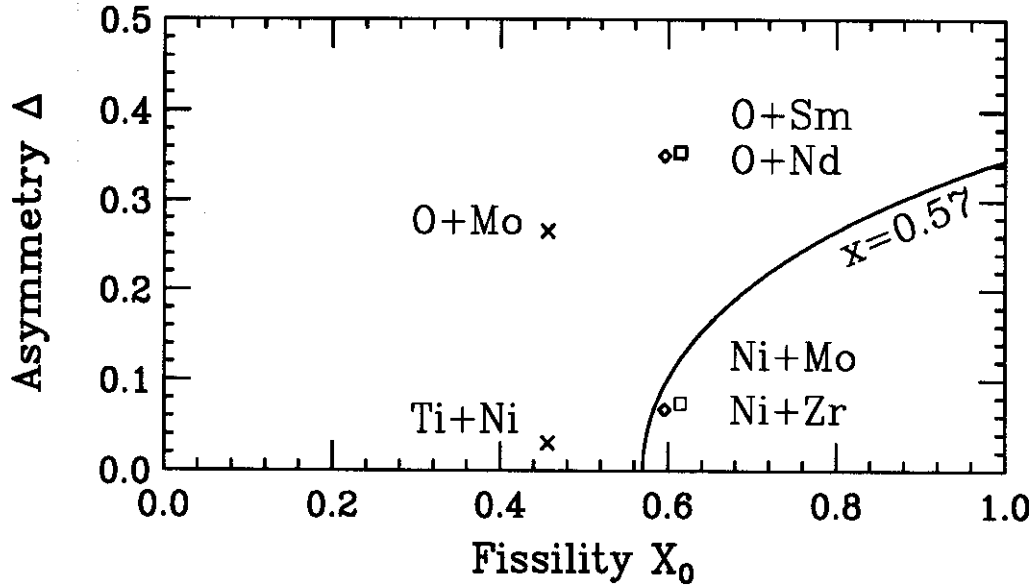


Figure 4: Classification of the reactions studied as a function of fissility X_0 and asymmetry Δ . To the right of the line $x = 0.57$ deep-inelastic reactions are expected to appear for central collisions.

his particle exchange model code HICOL.^{25,26} We use this code to calculate the time evolution of collisions. The code follows various important quantities of a reaction as a function of time. Figure 5 shows the shape evolution for the reactions $^{18}\text{O} + ^{92}\text{Mo}$, $^{50}\text{Ti} + ^{60}\text{Ni}$, $^{16}\text{O} + ^{148}\text{Sm}$, and $^{64}\text{Ni} + ^{100}\text{Mo}$ at an angular momentum of $25 \hbar$ corresponding to impact parameters of 3.9 fm, 2.6 fm, 3.3 fm and 1.5 fm respectively. The last column shows the $^{64}\text{Ni} + ^{100}\text{Mo}$ reaction at $29 \hbar$ (1.7 fm) and will be discussed later. The more symmetric reactions are clearly seen to be slower to evolve than the very asymmetric reactions. The important result is the time dependence of the shape evolution. Even though the impact parameters are smaller for the symmetric reactions it can be seen that they go through stages of much larger deformations. The $^{64}\text{Ni} + ^{100}\text{Mo}$ reaction takes much longer (about a factor of 5) to reach a shape equilibration that might be identified with a compound nucleus than the other three reactions, as predicted qualitatively by Fig. 4. Figure 6 shows the time evolution of some of the important quantities at the same angular momentum as in Fig. 5 ($25 \hbar$). The upper panel shows how fast the systems reach a thermal (effective excitation energy) equilibrium. The shape equilibration can be parameterized by the quadrupole moment (bottom) as a function of time.

These timescales can now be compared to the particle evaporation times of the compound nuclei in order to see if they are comparable or if they can be neglected. Since neutron decay is the dominant decay channel in these reactions, the average neutron life time can be taken as a characteristic life time. At an excitation energy of 56 MeV and 49 MeV for the ^{110}Sn and ^{164}Yb , respectively, the angular momentum averaged neutron lifetime is $270 \times 10^{-22}\text{s}$. Thus, this decay can be considered long

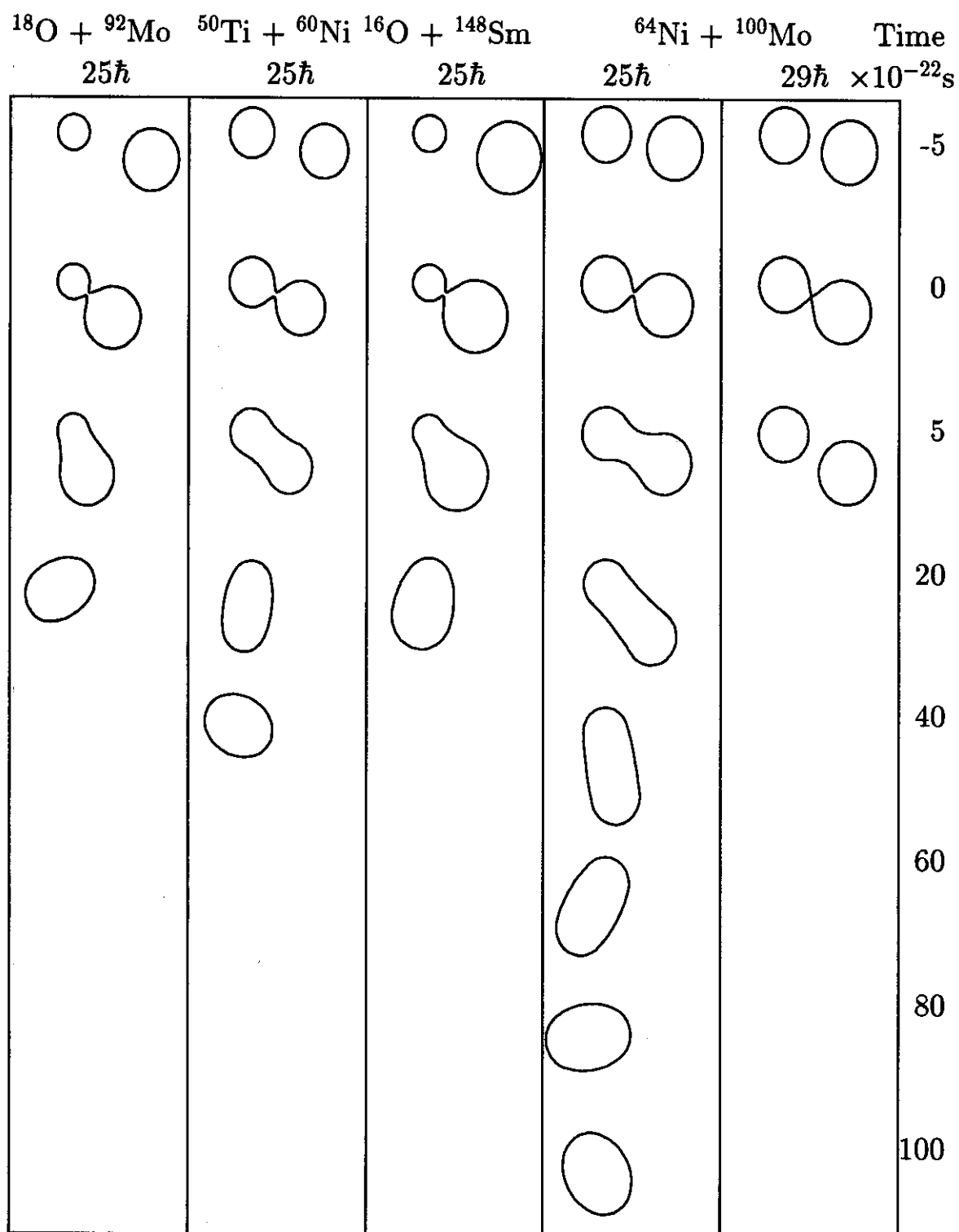


Figure 5: Time evolution of the reactions for an angular momentum of $25 \hbar$. The last column demonstrates a deep inelastic collision for $^{64}\text{Ni} + ^{100}\text{Mo}$ at $29 \hbar$.

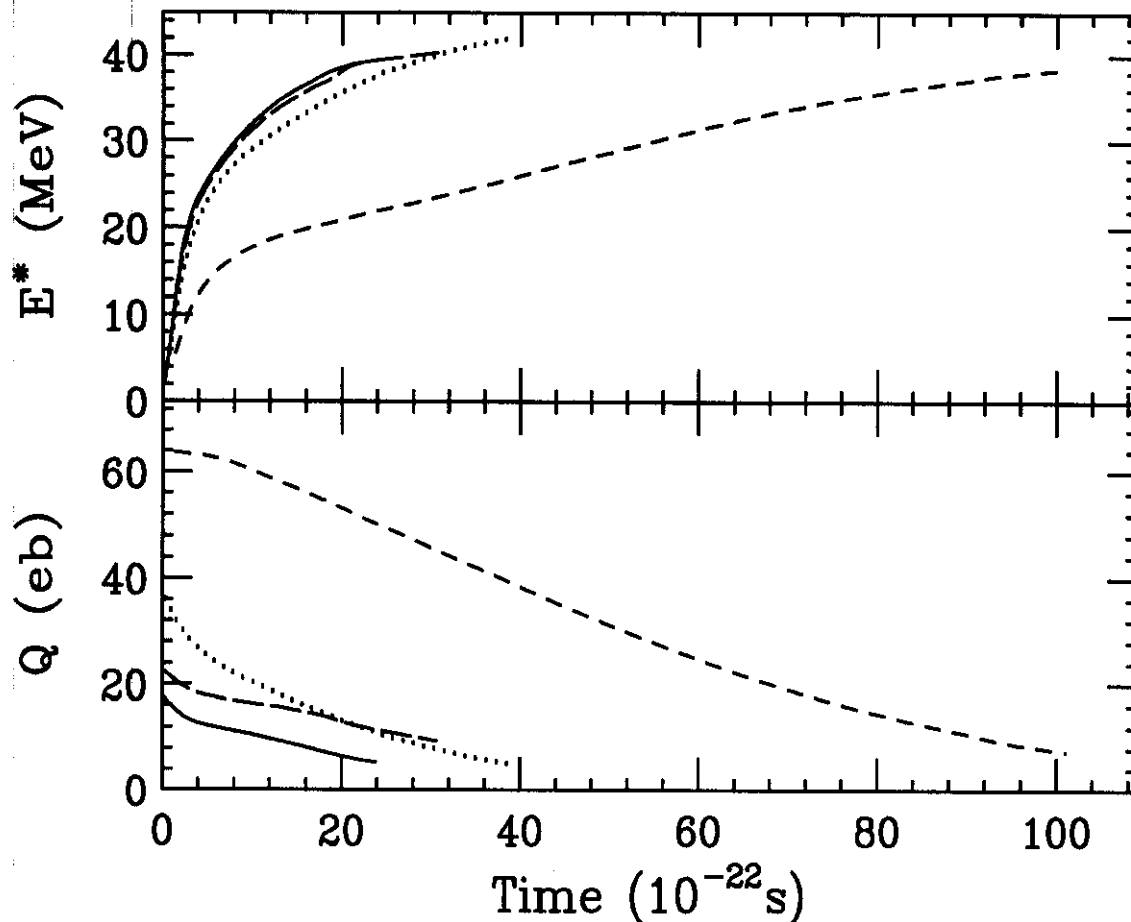


Figure 6: Evolution of excitation energy (top) and quadrupole moment (bottom) as a function of time for the reactions $^{18}\text{O} + ^{92}\text{Mo}$ (solid), $^{50}\text{Ti} + ^{60}\text{Ni}$ (dots), $^{16}\text{O} + ^{148}\text{Sm}$ (long-dashed), and $^{64}\text{Ni} + ^{100}\text{Mo}$ (short-dashed).

compared to the equilibration time of $\sim 20 \times 10^{-22}\text{s}$ for the asymmetric and $^{50}\text{Ti} + ^{60}\text{Ni}$ systems. This is certainly supported by experiment since all these reactions are described fairly well within the statistical model. However, the $^{64}\text{Ni} + ^{100}\text{Mo}$ reaction has an equilibration time at $l = 25 \hbar$ of $\sim 100 \times 10^{-22}\text{s}$ which is comparable to the neutron lifetime. One can try to estimate approximately the decay probability during equilibration. Under the assumption that the nucleus or more accurately the colliding dinuclear system can emit neutrons using the same parameters as in the equilibrated system, about 10% of all nuclei would emit a neutron before equilibration. However, in making this estimate we are applying an equilibrium statistical model to a non-equilibrated system which is at best questionable.

The fact that the $^{64}\text{Ni} + ^{100}\text{Mo}$ reaction takes about 5 times longer, suggests that particle/ γ -ray emission during that time could be possible. If that is the case it would certainly change the "initial" population of the compound nucleus by the time it is

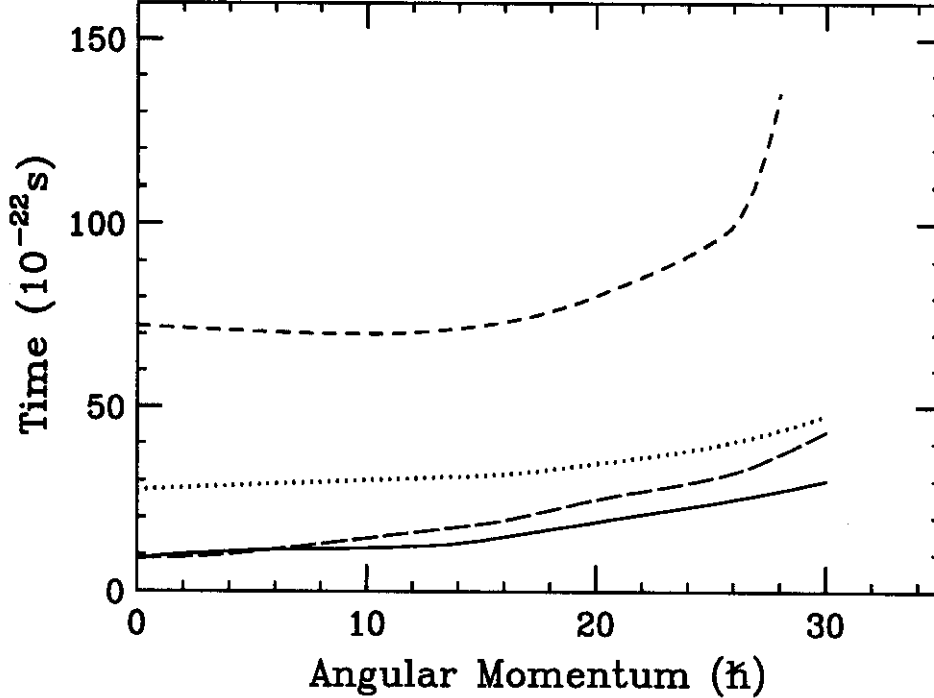


Figure 7: Compound nucleus formation time as a function of angular momentum for the reactions $^{18}\text{O} + ^{92}\text{Mo}$ (solid), $^{50}\text{Ti} + ^{60}\text{Ni}$ (dots), $^{16}\text{O} + ^{148}\text{Sm}$ (long-dashed), and $^{64}\text{Ni} + ^{100}\text{Mo}$ (short-dashed).

equilibrated. Thus the independence hypothesis might appear to be violated, though it is not, since when comparing the decay of compound nuclei formed in symmetric and asymmetric reactions, the compound nucleus population distribution is not the same by the time equilibrium is reached, due to particle and/or γ -ray emission during equilibration. The trend of the calculations certainly suggests the importance of dissipative dynamical effects to our experimental observations, however, it appears that the effective dynamical delay in equilibration predicted by the HICOL code is not large enough to account for the dramatic effects observed in our γ -ray spectra and in the neutron multiplicity data. Either the code under estimates the size of this effect, or some additional effect has to be considered.

In the context of this last point we will further discuss another aspect of the model calculations. The compound nuclei are formed with a broad distribution of angular momenta. Figure 7 shows, for the same four reactions as Fig. 6, the equilibration time as a function of angular momentum. While the $^{18}\text{O} + ^{92}\text{Mo}$ (solid), $^{50}\text{Ti} + ^{60}\text{Ni}$ (dots) and $^{16}\text{O} + ^{148}\text{Sm}$ (long-dashed) do not show a strong dependence of the equilibration time on the angular momentum, the $^{64}\text{Ni} + ^{100}\text{Mo}$ (short-dashed) reaction shows a different behaviour. The time increases dramatically with increasing angular momentum. The particle exchange model code provides a classical description of the collision, which under estimates the range of entrance channel angular momenta which lead to fusion in the $^{64}\text{Ni} + ^{100}\text{Mo}$ reaction. This is demonstrated in the

last column of Fig. 5, where the two nuclei do not fuse anymore at $29 \hbar$, instead they reseparate after a short interaction time. However, it is well known that in reactions at energies close to the barrier, especially involving projectiles as heavy as nickel, quantum mechanical coupled-channel and/or particle transfer effects enhance the fusion cross sections dramatically in certain cases, and allow fusion to occur for much larger angular momenta than predicted semi-classically.² This effect is seen in the experimentally derived fusion angular momentum distribution shown in Fig. 1, where the $^{64}\text{Ni} + ^{100}\text{Mo}$ reaction populates states well above spin $40 \hbar$ in contrast to the semiclassical limit of $28 \hbar$.

It would be extremely interesting to calculate the continuation of the curve in Fig. 7 for the $^{64}\text{Ni} + ^{100}\text{Mo}$ reaction to higher spin values. The trend of the curve in Fig. 7 certainly suggests an extremely steep increase of the equilibration time at larger angular momenta. Even though the angular momentum cut applied to our data is a window of $15 - 30 \hbar$, the γ -ray multiplicity on which it is based has a resolution of about 25%, so that we could expect significant influence on our spectra from beyond the semiclassical $28 \hbar$ limit to fusion.

5. Summary and Conclusions

We have presented γ -ray spectra from heavy-ion fusion evaporation reactions, which showed strong evidence for entrance channel effects. The particle exchange model was applied in order to give a qualitative description of the time evolution of the fusion process.

The dynamics of the fusion process seems to strongly influence the evolution of the system toward an equilibrated compound nucleus, and that this dynamics can depend strongly on the entrance channel. In order to explain the size of the observed effects, a dynamical model has to be developed that would allow for particle and/or γ -ray emission during the equilibration process. In this model one has to calculate the decay probabilities in a non-equilibrated system. It would have to account for the constantly changing deformation, level density, internal excitation energy and angular momentum.

6. Acknowledgements

The work presented here was done in collaboration with R. L. Auble, C. Baktash, F. E. Bertrand, M. L. Halbert, D. C. Hensley, D. J. Horen, P. Mueller, D. H. Olive, and R. L. Varner, *Oak Ridge National Laboratory*, E. Ramakrishnan, *Michigan State University*, D. G. Sarantites and D. W. Stracener, *Washington University*, and W. Spang, *KFA Jülich*. This work was partially supported by the Joint Institute for Heavy Ion Research, Oak Ridge, TN 37831 and the U.S. National Science Foundation under Grant No. PHY-89-13815. Oak Ridge National Laboratory is managed by Martin Marietta Energy Systems, Inc. under contract DE-AC05-84OR21400 with

the U.S. Department of Energy. We like to thank Hans Feldmeier for the particle exchange model code HICOL.

7. References

1. J. Blocki, J. Randrup, W. J. Swiatecki, and C. F. Tsang, *Ann. Phys. (N.Y.)* **105**, 427 (1977).
2. M. Beckerman, *Phys. Rep.* **B129**, 145 (1985).
3. S. Bjørnholm and W. J. Swiatecki, *Nucl. Phys.* **A391**, 471 (1982).
4. W. J. Swiatecki, *Physica Scripta* **24**, 113 (1981).
5. D. J. Hinde, H. Ogata, M. Tanaka, T. Shimoda, N. Takahashi, A. Shinohara, S. Wakamatsu, K. Katori, and H. Okamura, *Phys. Rev. C* **39**, 2268 (1989), and references therein.
6. P. Grangé, S. Hassani, H. A. Weidenmüller, A. Gavron, J. R. Nix, and A. J. Sierk, *Phys. Rev. C* **34**, 209 (1986).
7. W. Kühn, P. Chowdhury, R. V. F. Janssens, T. L. Khoo, F. Haas, J. Kasagi, and R. M. Ronningen, *Phys. Rev. Lett.* **51**, 1858 (1983).
8. R. V. F. Janssens, R. Holzmann, W. Henning, T. L. Khoo, K. T. Lesko, G. S. F. Stephans, D. C. Radford, A. M. van den Berg, W. Kühn, and R. M. Ronningen, *Phys. Lett.* **181B**, 16 (1986).
9. K. A. Snover, *Ann. Rev. Nucl. Part. Sci.* **36**, 545 (1986).
10. M. Jääskeläinen, D. G. Sarantitis, R. Woodward, F. A. Dilmanian, J. T. Hood, R. Jääskeläinen, D. C. Hensley, M. L. Halbert, and J. H. Barker, *Nucl. Instr. and Meth.* **A204**, 385 (1983).
11. M. L. Halbert, J. R. Beene, D. C. Hensley, K. Honkanen, T. M. Semkow, V. Abenante, D. G. Sarantitis, and Z. Li, *Phys. Rev. C* **40** 2558 (1989).
12. M. Thoennesen *et al.*, in "Nuclear Structure and Heavy Ion Dynamics 1990", Edited by R. R. Betts and J. J. Kolata, Institute of Physics Conference Series 109, Adam Hilger, 1991.
13. F. Pühlhofer, *Nucl. Phys.* **A260**, 276 (1977).
14. V. Metag, private communication.
15. B. Haas *et al.*, *Phys. Rev. Lett.* **54**, 398 (1985).
16. R. Brun, F. Bruyant, M. Maire, A. C. McPherson, and P. Zancarini, *GEANT3 Users Guide*, Data Handling Division DD/EE/84-1, CERN 1986.
17. D. R. Chakrabarty, M. Thoennesen, S. Sen, P. Paul, R. Butsch, and M. G. Herman, *Phys. Rev. C* **37**, 1437 (1988).
18. R. Bock *et al.*, *Nucl. Phys.* **A388**, 334 (1982).
19. A. Stolk, M. N. Harakeh, W. H. A. Hesselink, H. J. Hofmann, R. F. Noorman, J. P. S. van Schagen, Z. Sujkowski, H. Verheul, M. J. A. de Voigt, and D. J. P. Witte, *Phys. Rev. C* **40**, R2454 (1989).

20. B. Fornal *et al.*, Phys. Rev. C **42**, 1472 (1990).
21. R. Butsch, D. J. Hofman, C. P. Montoya, P. Paul, and M. Thoennessen, Phys. Rev. C **44**, 1515 (1991).
22. D. R. Chakrabarty, S. Sen, M. Thoennessen, N. Alamanos, P. Paul, R. Schicker, J. Stachel, and J. J. Gaardhøje, Phys. Rev. C **36**, 1886 (1987).
23. J. J. Gaardhøje, C. Ellegaard, B. Herskind, R. M. Diamond, M. A. Delaplanque, G. Dines, A. O. Macciavelli, and F. S. Stephens, Phys. Rev. Lett. **56**, 1783 (1986).
24. J. Blocki, H. Feldmeier, and W. J. Swiatecki, Nucl. Phys. **A459**, 145 (1986).
25. H. Feldmeier, Program HICOL (1986).
26. H. Feldmeier, Rep. Prog. Phys. **50**, 915 (1987).